PARTIAL CROSS SECTIONS AND DENSITY OF STATES EFFECTS

IN THE VALENCE BAND PHOTOEMISSION FROM SOLID NITROGEN

by

H.-J. Lau and J.-H. Fock

II. Institut für Experimentalphysik, Universität Hamburg

E.E. Koch

Hamburger Synchrotronstrahlungslabor HASYLAB at DESY

Partial cross sections and density of states effects

in the valence band photoemission from solid nitrogen[+]

H.-J. Lau and J.-H. Fock

II. Institut für Experimentalphysik, Universität Hamburg,

D-2000 Hamburg 50, BRD

and

E. E. Koch

Hamburger Synchrotronstrahlungslabor HASYLAB at DESY

D-2000 Hamburg 52, BRD

Abstract

Photoelectron energy distribution curves from solid nitrogen have been

measured for excitation energies ranging from threshold (14.2 eV) to

40 eV using Synchrotron Radiation. The partial cross sections for the

emission from the $3\sigma_g$, $1\pi_u$ and $2\sigma_u$ derived valence bands show pronounced

maxima 3.4 eV, 2.9 eV and 3.0 eV above the vacuum level respectively

which we interpret as being due to a high density of conduction band

final states. These states are closely related to the π_g^* negative-ion

shape resonance for molecular nitrogen.

1. Introduction

Since the first photoelectron energy distribution measurements for solid
N_2 [1] a number of experiments have been performed on solid N_2 [2, 3],
matrix isolated N_2 [3] and N_2 chemisorbed and physisorbed on metal surfaces
(e.g. Refs. 4 - 8). These experiments provide detailed information con-
cerning the valence bands derived from the outer filled molecular orbitals
(MO's) where a one-to-one correspondence between the valence bands of the
solid phase and the gas phase MO's was observed. The resulting binding
energy shifts derived from these measurements by comparing spectra from the
gaseous, solid and adsorbed phase have been discussed in quite some detail
(1 - 8). Valence energy band dispersions $E(\underline{k})$ have not yet been determined,
due to the inherent difficulties in preparing single crystalline samples.
To our knowledge there are also no band structure calculations available for
solid N_2 up to now.

Optical experiments on solid N_2 have mainly been concerned with the
discrete states below the ionization threshold (9, 10), but little is
known on the higher conduction band states. In this letter we report on
photoemission experiments with tunable synchrotron radiation in which we
follow the partial cross-sections for the initial bands as a function of
excitation energy, thereby gaining important information on the final states
in the conduction band.

2. Experimental Details

Angle integrated photoelectron energy distribution curves (EDC's) were
measured with a commercial double-pass cylindrical mirror analyzer (CMA).
The analyzer was operated in the retarding mode. Synchrotron radiation
from the 5 GeV electron storage ring DORIS at DESY monochromatized by the
3 m normal incidence monochromator HONORMI (11) in the new synchrotron
radiation laboratory HASYLAB in Hamburg served as a tunable light source.
The count-rates were about 10^4/sec for the N_2 valence bands with an overall
resolution (monochromator and electron energy analyzer) of 0.2 eV. This
resolution was in all cases sufficient for an accurate determination of
features in the EDC's which have typical widths of 0.8 - 1.0 eV (FWHM).

Research grade N_2 gas (L'Air Liquide 99.9992% purity) was condensed under UHV conditions (pressure before and after condensation 1 x 10^{-10} Torr) on a helium cooled gold substrate. The temperature of the substrate was approximately 25 K. At these temperatures the growth of polycrystalline films of the low temperature phase of N_2 is favored (12). To avoid charging problems during photoemission, the sample thickness was limited to roughly 10 nm.

For the determination of photoemission intensities the EDC's for each excitation energy have been normalized to the intensity of the photon flux impinging on the sample. Secondly a smooth structureless background was subtracted from direct emission peaks to account for electrons originating from the aged gold substrate and for scattered secondary electrons. Finally, the area under each primary emission peak in the EDC's was determined by fitting the experimentally determined three peak structure by Gaussians. It turned out that in all cases a fit with one Gaussian for each peak was sufficient (13).

The largest uncertainty in the cross-section determination rests in the unknown transmission function of the electron energy analyzer. The analyzer was always operated in the retarding mode with pass energies E_{pass} = 10 eV for hν $\leq$ 30 eV and E_p = 30 eV for hν > 25 eV, respectively. Both settings for E_{pass} gave the same relative cross-sections in the overlapping photon energy range. The sample area seen by the electron analyzer was in all cases larger than the illuminated spot on the sample (1 mm^2). Under these conditions we assume that at least for kinetic energies of the photoelectrons $E_{kin} \gtrsim$ 5 eV the transmission function of the electron analyzer was independent of the kinetic energy of the photoelectrons. For smaller kinetic energies it is likely that the transmission decreases, because of grid scattering (14) so that the EDC intensities at small energies are underestimated. In any case, it is our experience when comparing measurements for different substances that the unknown exact transmission function does not introduce sharp structures or peaks but in the worst case leads only to a distortion of the cross-section data. Thus we estimate the errors in the relative cross-sections to be up to 30% (13).

3. Results and Discussion

In Fig. 1 a family of EDC's is shown for solid N_2 at different photon energies. In this plot peaks originating from the same initial state, i.e.

having the same binding energy, move to higher kinetic energies when the photon energy is increased and thus follow the inclined lines. The three main peaks for direct emission from solid N_2 are clearly visible. Their vertical binding energies are 15.1 eV, 16.6 eV and 18.3 eV, respectively, with reference to the vacuum level (E_{VAC} = 0) of the sample.

There is a clear one-to-one correspondence to the gas phase spectrum of N_2 (15 - 19). Therefore it is easy to assign these peaks, in agreement with previous work (1 - 3) to the ionization of valence bands formed by the $3\sigma_g$, $1\pi_u$ and $2\sigma_u$ MO's of the N_2 molecule.

In the EDC obtained with hν = 40 eV two additional structures marked by CI are visible. They correspond to the configuration interaction peaks already known for gas phase N_2 (16, 17) and are observed here for the first time for the solid phase. The binding energies and widths (FWHM) of the valence bands are summarized in Table 1 where the gas phase results are given for comparison.

Here we are in particular interested in the hν -dependence of the partial photoionization cross-sections for the three valence bands. Inspection of Fig. 1 shows immediately that each of the primary peaks goes through a maximum at around 3 eV kinetic energy. The result of the detailed analysis is displayed in Fig. 2.

From the energy distribution curves, like those shown in Fig. 1, we obtain the relative partial ionisation cross-sections σ_i for the i-th level of the molecule by measuring the area A_i under each peak. We note in passing that this equation is only valid for an angle integrating geometry, since the number of photoemitted electrons detected for a given state i depends not only upon the partial photoionization cross-section σ_i but also upon the angle of collection Θ with respect to the direction of polarization. In the truly molecular case, the asymmetry parameter β_i characterizes the angular distribution of the i-th ionic state at a given photon energy (20). In our experiments where we measure angle integrated EDC's, the emitted photoelectrons can be regarded as an isotropic source (see also the detailed discussion of a similar analysis in Ref. 18).

Note that the partial ionisation cross-sections in Fig. 2 are in arbitrary units, but the ratio between them as well as their photon energy dependence can be easily determined. The changes with photon energy are quite dramatic.

For example, at 18 eV, emission out of the $1\pi_u$ valence band is only weak, whereas at 20 eV this band has gained considerably in intensity. A similar behaviour is observed for the other two bands.

It is interesting to compare the gas phase partial ionisation cross-sections (18, 19) for N_2 with our results. This comparison is shown in Fig. 2. For photon energies $\gtrsim$ 28 eV, both the gas phase and solid phase partial ionisation cross-sections σ_i become very similar. There are, however, marked differences for each band immediately above threshold. For gaseous N_2 the partial photoionisation cross-sections exhibit sharp structures due to autoionisation of Rydberg states near the ionisation thresholds (18, 19, 21). These intensity variations are also distributed in a striking non-Franck-Condon way among the individual vibrational bands of the ionic states (21). Thus, aside from the experimental problems in determining accurately photoemission intensities near threshold (see above), these interchannel interactions in the gas phase may obscure the prominent resonances observed here for the solid phase.

We attribute the strong resonances appearing for each photoemission band to the band structure of solid N_2. The N_2 valence bands are, as characteristic for an insulator, flat (FWHM $\sim$ 1.0 eV, see Table 1) and are expected to show only little dispersion. Thus, the maxima appearing for each partial ionisation cross-section can be explained by a high density of final conduction band states. This is schematically depicted in Fig. 3.

Our interpretation is supported by the observation of pronounced maxima of scattered electrons in each EDC peaking at $\sim$ 3.5 eV kinetic energy. These maxima of secondary electrons are nicely visible in the spectra for $h\nu \gtrsim$ 25 eV (Fig. 1) where they are almost not obscured by primary emission. They reflect the high density of final states into which primary electrons are scattered inelastically.

In molecular crystals, such as N_2, excitation of several electronic and vibrational excited states can contribute to electron scattering and we hence do not observe a sharp onset due to one single process dominating the electron scattering mechanism. This is different from the situation in rare

gas solids where electron exciton scattering characterized by a well defined excitation energy dominates the electron scattering process (22). In Fig. 3 we have schematically depicted a number of valence excitations for solid N_2 (9, 10) which, together with excitation of intramolecular vibrations and phonons can lead via inelastic scattering of the primary photoelectrons to secondary electrons of low kinetic energy. Thus, the intensity distribution of the scattered electrons is not dominated by one single scattering mechanism but largely reflects the density of final conduction band states.

Further support for our assignment comes from an analysis of the optical spectra of solid N_2 (9). Below the onset of photoemission at 15.1 eV, sharp excitonic structures dominate the optical spectrum. The broad optical transitions above this energy which peak at around 19.5 eV can, in view of the present results, be well described as valence to conduction band transitions. Indeed, the sum of the partial photoionisation cross-sections determined here reproduces quite well the broad maximum in the optical spectrum around 19 eV.

Finally, we want to comment on the nature of the resonance in the continuum for each valence band (Fig. 2), which we have hitherto discussed as the conduction band. What is the molecular origin of the states contributing to the conduction band density of states? It is well known from electron scattering experiments on gaseous N_2 that resonances dominate the electron-scattering cross-section (23). These resonances are temporarily negative ion resonances, where the incoming electron is trapped in a virtual bound state of the molecule. The nitrogen molecule has a strong π_g^* resonance near 2.3 eV with a negative ion lifetime of $\sim 10^{-14}$ sec. (23) and a broad resonance around 22 eV which is assigned to the σ_u^* channel (24). In photoemission experiments the analogue to these negative ion resonances has been discussed as shape resonances (25, 26) and Dill and Dehmer (25) as well as Davenport et al. (26) have shown for diatomic molecules that these resonant states in the continuum can be well treated by a multiple scattering formalism. But up to now for photoionisation only the σ_u^* shape resonance derived from the 3 σ_u^* virtual orbital has been calculated and observed for ionisation out of the 3 σ_g valence orbital of gaseous N_2 (18, 19, 24-26).

On the other hand we expect a π_g^* resonance also in photoionisation, in complete analogy to the electron scattering case. As a matter of fact, Dehmer and Dill (25) find such a resonance in the π_g-channel in K-shell photoionisation. But in this case the molecular potential is more attractive, because of the core hole and the resonance is therefore shifted into the discrete spectrum.

For valence shell photoionisation the situation is more complicated, since only small changes in the molecular potential can shift the resonance from the discrete to the continuous spectrum (27). Moreover, because of the presence of the strong b' $^1\Sigma_u^+$ ← X $^1\Sigma_g^+$ valence transition a good configuration - interaction calculation would be needed, in order to determine properly the details of the photoionisation cross section near threshold. For the solid phase the hole can be screened effectively by the surrounding medium. Thus, it is likely that the π_g resonance is shifted to higher energies and is now amenable to observation in photoemission. Hence, in a band structure language, the molecular $1\pi_g^*$ virtual orbital gives rise to a high density of conduction band states in the solid. Since we are dealing with solid N_2 the molecular selection rules do not apply strictly and we observe the resonance for emission out of all three valence bands. The $1\pi_u \rightarrow 1\pi_g^*$ transition is, in accord with our observations, expected to be strong due to the d-wave character of the π^*-resonance (26).

In conclusion, we have traced back the resonances appearing in the partial photoionisation cross-sections from the valence bands of solid N_2 to maxima in the conduction band density of states which have their origin in the π^* resonance of molecular N_2. Our results suggest that these resonances are a common feature of photoemission from molecular crystals formed by molecules which show pronounced shape resonances in the gas phase.

References

Work supported in part by Bundesministerium für Forschung und Technologie (BMFT) from Funds for Research with Synchrotron Radiation

1 F.-J. Himpsel, N. Schwentner and E.E. Koch, phys. stat. sol. b 71, 615 (1975)

2 P.R. Norton, R.L. Trapping, H.P. Broida, J.W. Gadzuk and B.J. Waclawski, Chem. Phys. Lett. 53, 465 (1978)

3 D. Schmeisser and K. Jacobi, Chem. Phys. Lett. 62, 51 (1979)

4 J.C. Fuggle and D. Menzel, Proc. 7th Int. Vacuum Congress and 3rd Int. Conf. on Solid Surfaces, Vienna 1977, p. 1003.

5 J.C. Fuggle and D. Menzel, Vakuum Technik 27, 130 (1978)

6 E. Umbach, A. Schichl and D. Menzel, Solid State Comm. 36, 93 (1980)

7 P.S. Bagus, C.R. Brundle, K. Hermann and D. Menzel, J. Electr. Spectr. 20, 253 (1980)

8 K. Horn, J. DiNardo, W. Eberhardt, H.J. Freund and E.W. Plummer, preprint August 1981.

9 R. Haensel, E.E. Koch, N. Kosuch, U. Nielsen and M. Skibowski, Chem. Phys. Lett. 9, 548 (1971) and references therein.

10 P. Gürtler and E.E. Koch, Chem. Phys. 49, 305 (1980) and references therein.

11 V. Saile, P. Gürtler, E.E. Koch, A. Kozevnikov, M. Skibowski and W. Steinmann, Appl. Optics 15, 2559 (1976)

12 W. Schulze, D.M. Kolb and G. Klipping, J. Chem. Soc. Faraday II, 1098 (1974)

13 H.-J. Lau, Diplomarbeit, Universität Hamburg, 1982.

14 P.W. Palmberg, J. Vac. Sci. Technol. 12, 379 (1975)

15   D.W. Turner, C. Baker, A.D. Baker and C.R. Brundle, Molecular
     Photoelectron Spectroscopy, Wiley, London 1970.

16   K. Siegbahn et al., ESCA Applied to Free Molecules, North Holland
     Publishing Company, Amsterdam 1971.

17   A.W. Potts and T.A. Williams, J. Electr. Spectr. 3, 3 (1974).

18   E.W. Plummer, T. Gustafsson, W. Gudat and D.E. Eastman, Phys. Rev. A
     15, 2339 (1977)

19   P.R. Woodruff and G.V. Marr, Proc. R. Soc. Lond. A 358, 87 (1977)

20   C.N. Yang, Phys. Rev. 74, 764 (1948)

21   W.B. Peatman, B. Gotchev, P. Gürtler, E.E. Koch and V. Saile,
     J. Chem. Phys. 69, 2089 (1978) and

     A.C. Parr, D.L. Ederer, B.E. Cole, J.B. West, R. Stockbauer, K.
     Codling and J.L. Dehmer, Phys. Rev. Lett. 46, 22 (1981) and references
     therein.

22   N. Schwentner, E.E. Koch and J. Jortner, in: Rare Gas Solids, ed. by
     M.J. Klein and J. Venables, Academic Press, New York, in press.

23   G.J. Schulz, Rev. Mod. Phys. 45, 423 (1973)

24   J.L. Dehmer, J. Siegel, J. Welch and D. Dill, Phys. Rev. A 21, 101
     (1980)

25   D. Dill and J.L. Dehmer, J. Chem. Phys. 61, 692 (1974);
     Phys. Rev. A 1b, 1423 (1977); J. L. Dehmer and D. Dill, Phys. Rev.
     Lett. 35, 213 (1975); J. Chem. Phys. 65, 5327 (1976).

26   J.W. Davenport, Phys. Rev. Lett. 36, 945 (1976);
     J.W. Davenport, W. Ho and J.R. Schrieffer, Phys. Rev. B 17, 3115 (1978)

27   T.N. Rescingo, C.F. Bender, B.V. McKoy and P.W. Langhoff, J. Chem.
     Phys. 68, 970 (1978); T.N. Rescingo, A. Gerwer, B.V. McKoy and P.W.
     Langhoff, Chem. Phys. Lett. 66, 116 (1979)

Table 1:

Experimentally determined energies describing the band structure of solid N_2.
The zero of the energy scales is the vacuum level of the sample ($E_{VAC} = 0$).
Following the MO convention, the binding energies of occupied bands are given
as positive numbers. The estimated error is $\pm$ 0.15 eV. The adiabatic binding
energies E_B^{ad} have been determined by fitting the experimental curve for each
band with a Gaussian line shape and by using $E_B^{ad} = E_B^{v} - 1.2\Gamma$; E_B^{v}: vertical
bindung energy; Γ: half width (FWHM). Gas phase values are given for comparison.

Band / Orbital	Symmetry	Binding Energies			
		Solid[a]			Gas
		E_B^{ad}	E_B^{v}	FWHM	E_B^{v}
center of conduction band	$1\pi_g^{*}$		-3.1		-2.3[b]
valence bands	$3\sigma_g$ $(X^2\Sigma_g^{+})$	14.2	15.1	0.75	15.6[c]
	$1\pi_u$ $(A^2\Pi_u)$	15.3	16.6	1.05	16.98[c]
	$2\sigma_u$ $(B^2\Sigma_u^{+})$	17.8	18.3	0.80	18.78[c]
	CI $(C^2\Sigma_u^{+})$		25.0		25.3[d]
	CI		28.0		28.8[d]

References

a)   This work

b)   G.J. Schulz, Rev. Mod. Phys. 45, 423 (1973)

c)   D.W. Turner, C. Baker, A.D. Baker and C.R. Brundle,
     Molecular Photoelectron Spectroscopy, Wiley, 1970

d)   A.W. Potts and T.A. Williams, J.Electr.Spectr. 3, 3 (1974)

Figure Captions

Fig. 1   Photoelectron energy distribution curves for polycrystalline solid N_2 for excitation energies between 15 eV and 40 eV. In this plot the same initial states follow inclined lines. The three valence molecular orbitals are denoted by the one electron MO notation. In the 40 eV spectrum structures due to configuration interaction are marked by CI.

Fig. 2   Relative partial ionisation cross-sections for the $3\sigma_g$-derived, $1\pi_u$ derived and $2\sigma_u$ derived valence bands of solid N_2 (full curves). The arrows mark the onset for photoemission from these bands. For comparison the partial cross-sections for gaseous N_2 (18) are shown (crosses) which have been scaled for $h\nu = 30$ eV for the $3\sigma_g$ band and enlarged by a factor of 10.

Fig. 3   Schematic energy scheme for the occupied valence MO's and valence bands VB's in gaseous and solid N_2 respectively. For gaseous N_2 the $1\pi_g^*$ negative ion shape resonance above the vacuum level is shown. It corresponds to the maximum of the conduction band (CB) density of states for solid N_2 (see text).
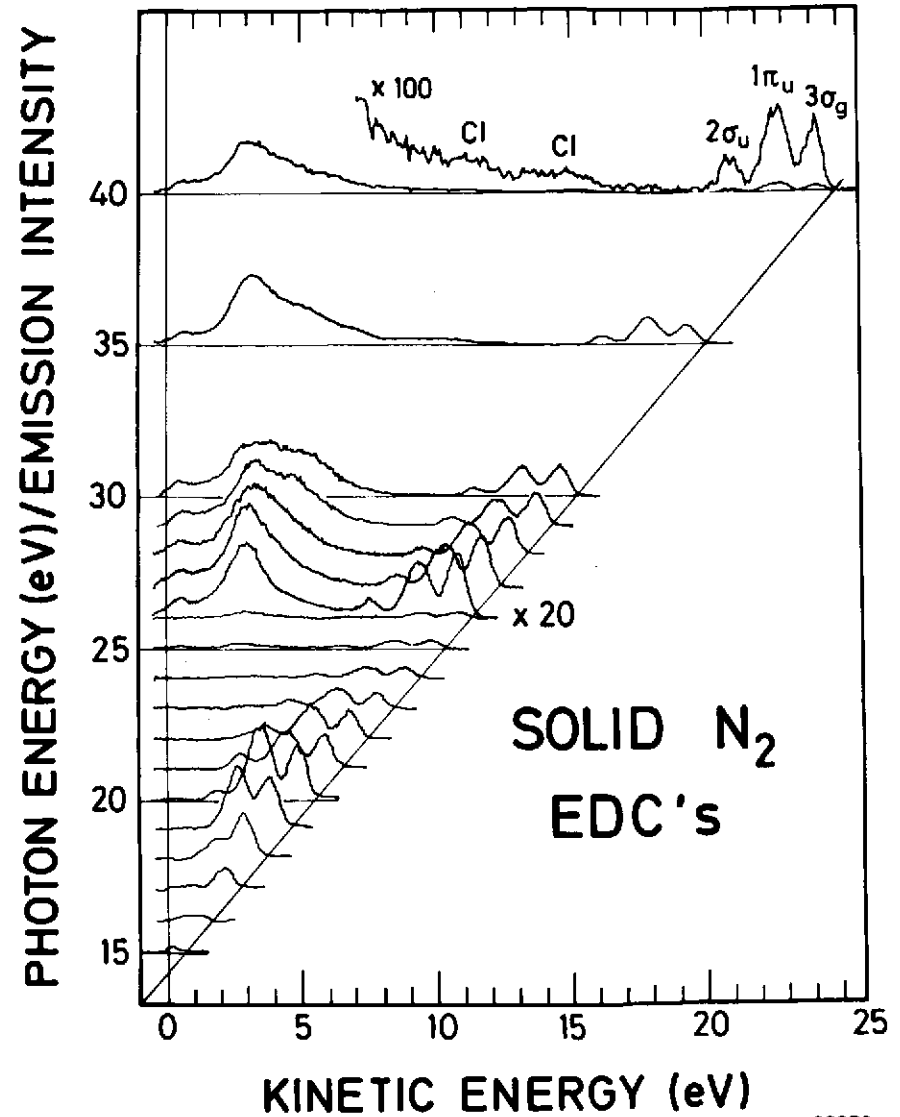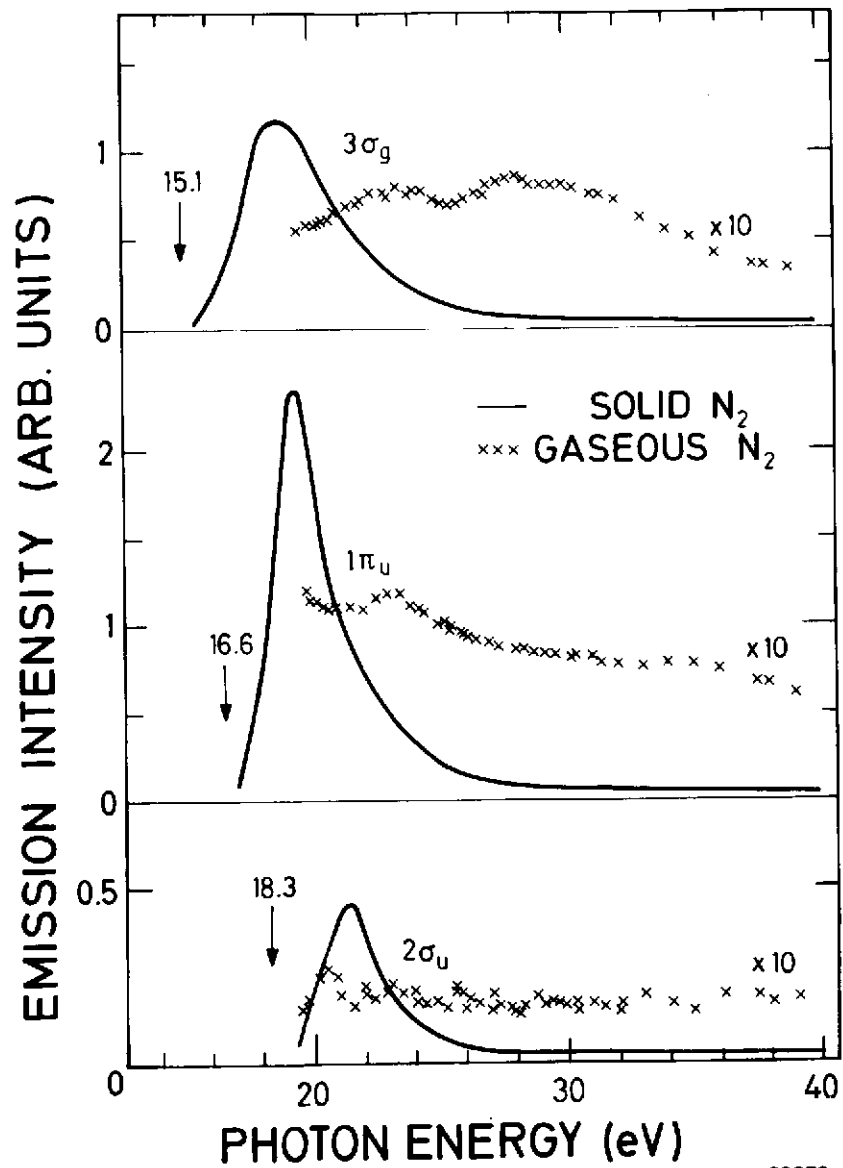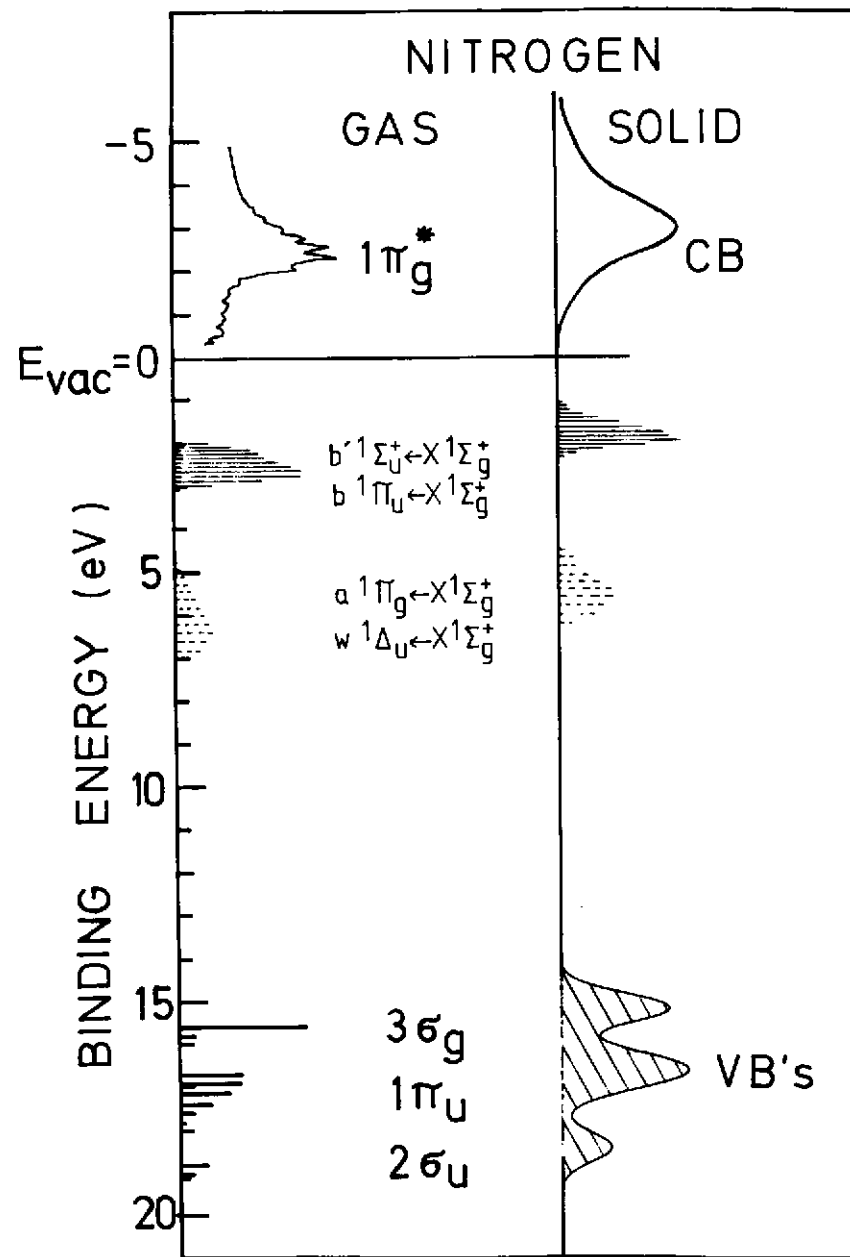

Fig. 1

Fig. 2

Fig. 3